

## Resistive transition, magnetoresistance, and anisotropy in $\text{La}_{2-x}\text{Sr}_x\text{CuO}_4$ single-crystal thin films

Minoru Suzuki and Makoto Hikita\*

*NTT Applied Electronics Laboratories, NTT Ibaraki Research and Development Center,  
Nippon Telegraph and Telephone Corporation, 162 Tokai, Ibaraki 319-11, Japan*

(Received 20 December 1990)

The temperature dependence of the resistivity  $\rho(T)$  in the vicinity of the superconducting transition temperature  $T_c$  has been measured for thin-film single crystals of  $\text{La}_{2-x}\text{Sr}_x\text{CuO}_4$  as a function of an applied magnetic field, both parallel and perpendicular to the  $c$  axis. The resistive transition exhibits characteristic behavior, depending on the Sr concentration  $x$ , when a field is applied. For small  $x$  the application of a field causes a significant broadening of the resistive transition—a behavior thought to be typical of high- $T_c$  cuprate superconductors—while for  $x$  exceeding 0.15, it simply causes a parallel shift of the curves to lower temperatures. From the analysis of the magnetoresistance above  $T_c$  based on the theory of field-dependent fluctuation conductivity for layered materials, it is shown that the behavior of the field-induced resistive transition can be ascribed to the flux motion, especially when  $H \perp c$ . The analysis also shows that the out-of-plane Ginzburg-Landau coherence length  $\xi_c(0)$  increases systematically with  $x$  from 0.55 Å at  $x=0.08$  to 3 Å at  $x=0.3$ , while the in-plane Ginzburg-Landau coherence length  $\xi_{ab}(0)$  is almost constant and  $\xi_{ab}(0)=31-33$  Å, irrespective of the value of  $x$  as long as  $T_c$  remains high. The anisotropy  $\xi_{ab}(0)/\xi_c(0)$  estimated from these results exceeds 50 at low Sr concentrations and is still larger than 15 even for  $x > 0.1$ .

### I. INTRODUCTION

To shed light on the nature and origin of high- $T_c$  superconductivity in cuprates, it is of significant importance to know accurate values for superconducting properties including coherence lengths  $\xi$  or upper critical fields  $H_{c2}$ , by which one can gain an insight into the fundamental microscopic parameters of the superconductors. Usually coherence lengths are directly obtainable by measuring  $H_{c2}$ , i.e., ordinarily by observing the shifts of the resistive transition curves as a function of an applied field. In high- $T_c$  superconductors, however, estimating  $H_{c2}$  values by such a conventional resistive method is difficult due to the field-induced broadening of resistive transition,<sup>1,2</sup> which masks the true shift of  $T_c$  under magnetic fields.

In high- $T_c$  superconductors, the application of a magnetic field causes a pronounced broadening of resistive transition.<sup>1-7</sup> The above-mentioned difficulty in the resistive approach to  $H_{c2}$  is inherent to high- $T_c$  superconductors, which are characterized by a structure consisting of electrically conducting  $\text{CuO}_2$  layers. At the earliest stages in the study of high- $T_c$  superconductors, specimen inhomogeneity was invoked to explain this anomalous broadening. Soon thereafter single crystals of high quality became available, however; these observations were then ascribed to anomalously large flux creep and flow phenomena or giant flux creep by Yeshurun and Malozemoff.<sup>3</sup> Also, the observation of thermally activated resistive behavior in the Bi-Sr-Ca-Cu-O system by Palstra *et al.*<sup>4</sup> revealed that very short coherence length reduces the pinning energy, enhancing motion of flux lines at high temperatures, and causing resistivity due to their dissipative flux motion. Consequently, the short-

ness of the coherence length itself makes it very difficult to determine its value accurately. The  $H_{c2}$  or  $\xi$  values so far estimated using the resistive method are thus questionable.

Concerning causes for the broadening, explanations have been attempted other than the dissipation due to flux motion. Tsuneto<sup>8</sup> and Ikeda, Ohmi, and Tsuneto<sup>9</sup> calculated resistive transition curves induced by a field based on the renormalized fluctuation theory, and explained the resistivity  $\rho$  in a limited region below  $T_c$  for  $\text{Ba}_2\text{YCu}_3\text{O}_{7-y}$ . Oh *et al.*<sup>10</sup> attempted to interpret the broadening of resistive transition in terms of critical fluctuation. Thus the resistive behavior under fields below and close to  $T_c$  is still an issue and is yet to be explained, though it is likely that the dissipation due to flux motion is dominant in the region where  $\rho \rightarrow 0$ .

Taking this anomalous resistive behavior into account, several approaches to  $H_{c2}$  values have been proposed. Welp *et al.*<sup>11</sup> attempted to determine the  $H_{c2}$  values for  $\text{Ba}_2\text{YCu}_3\text{O}_{7-y}$  by observing a linear-in-temperature part of the magnetization in the vicinity of  $T_c$ , which results from the Ginzburg-Landau (GL) theory. Another method by Suzuki and Hikita<sup>12</sup> utilized the temperature dependence of the thermally activated resistive transition, which scales with the  $n$ th power of  $1-t$ , where  $t = T/T_c(H)$  is the reduced temperature. These methods are essentially the same in that the  $(1-t)^n$  dependence is taken into consideration in the vicinity of  $T_c$  based on the GL theory.

While the resistive behavior below  $T_c$  is subject to the influence of flux motion, resistivity  $\rho$  above the thermodynamic  $T_c$  is free from it. The methods in which superconducting fluctuation is involved take this advantage. Matsuda *et al.*<sup>13</sup> and Hikita and Suzuki<sup>14</sup> have estimated

values for  $\xi$  for  $\text{Ba}_2\text{YCu}_3\text{O}_{7-y}$  from the fluctuation conductivity above the thermodynamic  $T_c$  or mean-field  $T_c^{\text{mf}}$ , obtaining values of  $\xi_{ab}(0) = 11.5 \pm 0.5 \text{ \AA}$  and  $\xi_c(0) = 1.5 \pm 0.5 \text{ \AA}$ .

In the present study we have measured resistive transitions under fields in the  $\text{La}_{2-x}\text{Sr}_x\text{CuO}_4$  system, a prototype material for understanding the mechanism of high- $T_c$  superconductivity, and estimated coherence lengths and anisotropy as a function of the Sr concentration  $x$ , covering a wide compositional range from  $x = 0.08$  to  $0.3$ , by the method of analyzing fluctuation-induced magnetoresistance above  $T_c$ . It is found that the values for coherence lengths and anisotropy factor thus obtained are totally different from those estimated resistively,<sup>15</sup> though there are a few reports describing coherence lengths and anisotropy factor of  $\text{La}_{2-x}\text{Sr}_x\text{CuO}_4$  and the data are available only in a limited compositional range. It is shown that with increasing  $x$  the out-of-plane coherence length  $\xi_c(0)$  increases systematically from  $0.55 \text{ \AA}$  at  $x = 0.08$  to  $3 \text{ \AA}$  at  $x = 0.3$ , while the in-plane coherence length  $\xi_{ab}(0)$  is almost constant irrespective of  $x$  as long as  $T_c$  remains high. The anisotropy of the electronic structure estimated from these results exceeds 50 at a low Sr concentration and is still larger than 15 even for  $x > 0.1$ . We discuss these results in relation to the dimensionality and the abrupt disappearance of superconductivity at  $x = 0.3$ . We also show that the behavior of resistive transition induced by a magnetic field changes systematically from the broadening to the parallel shift behavior as  $x$  increases. We compare these results with the consequence of fluctuation analysis.

In relation to the origin of high- $T_c$  superconductivity or its dimensionality, determining anisotropy factor is also important. Recently Iye *et al.*<sup>16</sup> have revealed, by improving their measurement method, that anisotropy of the Bi-Sr-Ca-Cu-O system is significantly higher than the earlier results. In the present study we also show that the anisotropy factor in the  $\text{La}_{2-x}\text{Sr}_x\text{CuO}_4$  system is much larger than the values previously estimated.

The organization of the present paper is as follows. Section II deals with experimental details. Comprehensive experimental data on the resistive transition curves induced by a magnetic field are accumulated in Sec. III. The analytical method of the magnetoresistance based on the field-dependent fluctuation conductivity is explained in Sec. IV, followed by discussions on resistive transition and the coherence lengths in Sec. V.

## II. EXPERIMENTAL DETAILS

### A. Sample preparation

Samples measured are  $\text{La}_{2-x}\text{Sr}_x\text{CuO}_4$  single-crystal thin films. Sample preparation details were reported elsewhere.<sup>17</sup> In brief, thin films were epitaxially grown on  $\text{SrTiO}_3$  (100) single-crystal substrates heated at about  $800^\circ\text{C}$  by rf single-target magnetron sputtering. To attain stoichiometry of the films, targets were enriched with CuO by 20%. It is shown by Rutherford backscattering and channeling analysis, x-ray diffraction analysis, and reflection high-energy electron diffraction (RHEED) ob-

servation that the films are single crystalline with the  $c$  axis perpendicular to the substrates. Since in the present study the determination of the true anisotropic properties is of primary importance, particular attention was paid to exclude specimens which include crystallographically misaligned grains or other phase ingredients.

There is an issue that the  $\text{La}_{2-x}\text{Sr}_x\text{CuO}_4$  system has only one single-phase composition at  $x \sim 0.15$  and specimens having other compositions are electronically inhomogeneous mixtures of superconducting and nonsuperconducting phases.<sup>18</sup> This argument is based on the  $x$  dependence of the Meissner fraction, which peaks at  $x \sim 0.15$ . No crystallographic evidence for the phase separation, however, has been provided except for high-pressure synthesized  $\text{La}_2\text{CuO}_{4+\delta}$  (Ref. 19). For our single-crystalline thin films, the (00 $l$ ) reflection peaks were examined and no trace of phase separation was found within our instrumental limit. The mean FWHM of, e.g., the (006) reflection peak was  $0.246^\circ$  with a standard deviation of  $0.0223^\circ$ , showing no shoulders nor noticeable increase in the FWHM when  $x$  increases or decreases from 0.15. Unlike polycrystalline specimens, such phase separation, if it exists, is unlikely in single-crystalline specimens, as in the present case.

Films were patterned into a rectangular shape, typically  $4.6 \times 0.8 \text{ mm}^2$ , with 8 terminals extending to electrode pads. Silver wires  $50 \mu\text{m}$  in diameter were used for leads and attached to samples with silver paste, followed by heat treatment at  $400^\circ\text{C}$  for 0.5 h.

From the specimens thus carefully chosen, more than 25 samples were taken for the measurements of resistive transitions under magnetic fields with the field direction parallel and perpendicular to the  $c$  axis. At each Sr composition  $x$ , at least two samples were taken for the measurements to confirm that the properties observed are intrinsic to the composition. Figure 1 shows the tempera-

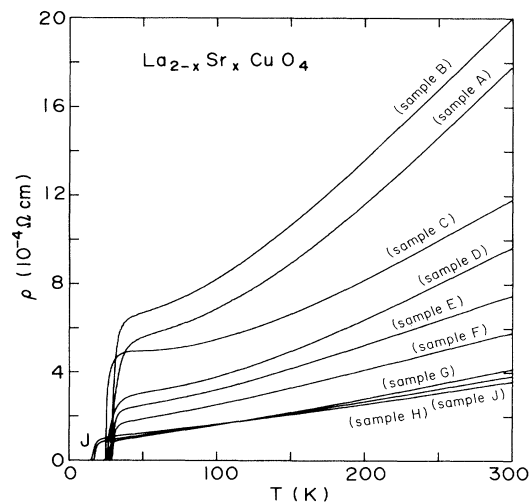


FIG. 1. Temperature dependence of the resistivity  $\rho(T)$  for  $\text{La}_{2-x}\text{Sr}_x\text{CuO}_4$  single-crystal thin films used in the present study for various Sr concentrations. Samples are labeled from A to J for convenience. Several physical properties are also listed in Table I.

ture dependence of the resistivity  $\rho(T)$  for representative samples chosen in this way. The composition  $x$  varies from 0.08 to 0.3 and the samples are labeled from *A* to *J*.

### B. Transport measurements

The resistivity was measured with a rotating sample holder in a superconducting solenoid which generates a field up to 12 T. Temperatures were determined with a carbon glass thermometer with detailed correction for magnetoresistance.<sup>20</sup> Resistivity was measured in the vicinity of the superconducting transition temperature  $T_c$  as a function of a field  $\mathbf{H}$ , both parallel and perpendicular to the  $c$  axis. Prior to the measurements, sample alignment was carefully adjusted under a field by rotating a sample around the angle where the  $\text{CuO}_2$  planes become parallel to a magnetic field.

Field-induced resistive transition curves were measured with a digital nanovoltmeter by scanning temperature very slowly under a fixed magnetic field. Using these data, magnetoresistance values at given temperatures were calculated by the spline interpolation method.

### III. RESISTIVE TRANSITION

As commonly observed in high- $T_c$  cuprate superconductors, applying a magnetic field causes a profound

broadening of the resistive transition also in the  $\text{La}_{2-x}\text{Sr}_x\text{CuO}_4$  system.<sup>6,7</sup> In this system, however, the way of broadening varies quite characteristically with the Sr content.<sup>7</sup> In a lightly doped region, as shown in Fig. 2 for the case of  $x=0.08$ , resistive transition exhibits a significant broadening under fields. In particular, this is conspicuous when a field is parallel to the  $c$  axis ( $\mathbf{H}\parallel c$ ). When a field is perpendicular to the  $c$  axis ( $\mathbf{H}\perp c$ ), the broadening is observed only in a region of  $\rho\sim 0$ , and little change is seen in the resistive transition curve for  $\rho>0.5\rho_n$ , where  $\rho_n$  is the normal resistivity, clearly reflecting that the  $\text{La}_{2-x}\text{Sr}_x\text{CuO}_4$  system is highly two dimensional (2D).

As the Sr concentration is increased from 0.1 to 0.15, resistive transition starts to change the way of broadening in a systematic way. In Figs. 3 and 4, resistive transition curves under fields are shown for  $x=0.1$  and 0.15, respectively.<sup>21</sup> Thus the field-induced broadening of resistive curves becomes modest as  $x$  increases. Kitazawa and co-workers<sup>6</sup> also reported characteristics similar to those of Fig. 3 for a  $\text{La}_{1.86}\text{Sr}_{0.14}\text{CuO}_4$  bulk single crystal. Similarly in Fig. 5–7, resistive transition curves are shown for  $x=0.2, 0.24,$  and  $0.3,$  respectively. For these compositions,  $T_c$  of the samples ranges from 17 to 30 K, depending on  $x$ . However, the behavior of the resistive transition under fields is almost the same irrespective of a value

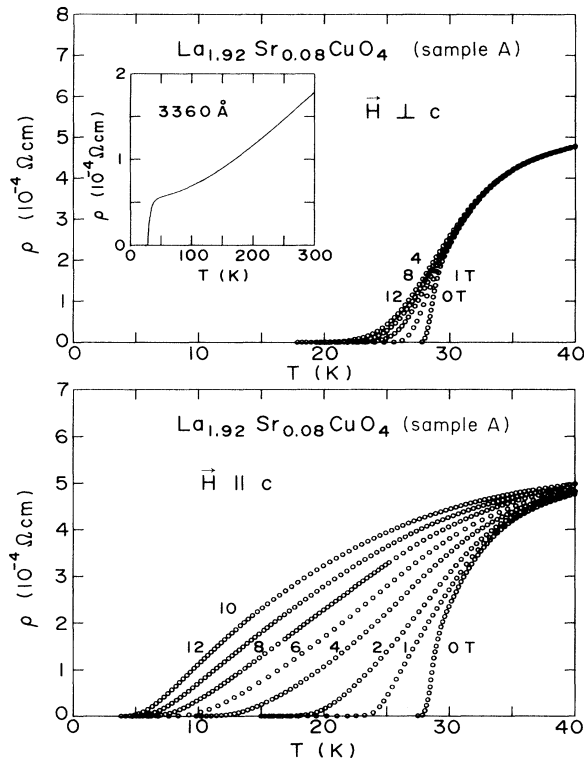


FIG. 2. Resistive transition curves for a  $\text{La}_{1.92}\text{Sr}_{0.08}\text{CuO}_4$  single-crystal thin film (sample *A*) under various applied magnetic fields from 1 to 12 T with the field direction perpendicular to the  $c$  axis (upper panel) and parallel to the  $c$  axis (lower panel). The inset into the upper panel shows an extended view of  $\rho(T)$ .

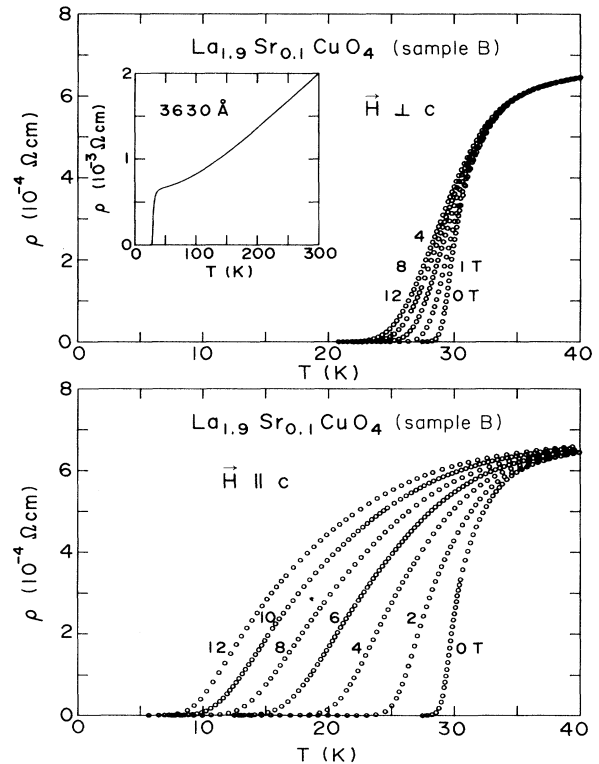


FIG. 3. Resistive transition curves for a  $\text{La}_{1.9}\text{Sr}_{0.1}\text{CuO}_4$  single-crystal thin film (sample *B*) under various applied magnetic fields from 1 to 12 T with the field direction perpendicular to the  $c$  axis (upper panel) and parallel to the  $c$  axis (lower panel). The inset into the upper panel shows an extended view of  $\rho(T)$ .

for  $T_c$ . For these compositions, applying a field causes almost no broadening and, instead, it causes a parallel shift of the curves to lower temperatures. This behavior clearly contrasts with that shown in Figs. 2–4.

The parallel shift behavior shown in Figs. 5–7 resembles that of conventional type-II superconductors, where the shift of the curves under fields directly corresponds to the shift of  $T_c$ , by which the values for  $H_{c2}$  are directly determined. If we simply apply this method to the present case for the  $\text{La}_{2-x}\text{Sr}_x\text{CuO}_4$  system and define  $T_c(H)$ , e.g., at the midpoint of the resistive transition, we obtain “ $H_{c2}$ ” values, which do not necessarily coincide with  $H_{c2}$ . These values are seriously underestimated because the resistive transition is for the most part caused by the energy dissipation due to vortex motion and the shift of the transition curves is much larger than the  $T_c$  shift. In Fig. 8 we plot these values for “ $H_{c2}$ ” or  $H'$  as a function of reduced temperature  $t = T_c(H)/T_c(0)$ . It is interesting to note that the curvature of  $H'-T$  plots for  $\mathbf{H}\parallel c$  changes from the minus to the plus as  $x$  increases. This eventually causes a linear portion near  $T_c$  for  $x=0.15$ . The negative curvature of such  $H'-T$  plots is also found in  $\text{Ba}_2\text{YCu}_3\text{O}_{7-y}$  when  $T_c$  is defined at a larger fraction of  $\rho_n$  in the resistive transition.<sup>22</sup> For  $\mathbf{H}\perp c$ , the curvature is positive irrespective of  $x$  values,

and the shift of the curves becomes larger as  $x$  increases. This behavior, together with the almost invariant behavior of the  $H'-t$  plots for  $\mathbf{H}\parallel c$ , appears to imply that the anisotropy of  $H_{c2}$  or the electronic structure of the  $\text{La}_{2-x}\text{Sr}_x\text{CuO}_4$  system changes systematically as the Sr doping. Indeed, when  $x$  is small, the slope of  $H'-t$  plots for  $\mathbf{H}\perp c$  is significantly large, probably reflecting the large anisotropy of more than 50. For  $x > 0.15$ , however, we should not rely on these plots in estimating  $H_{c2}$  values or electronic anisotropy, as will be explained in Sec. V.

## IV. MAGNETORESISTANCE

### A. Anisotropic magnetoresistance

Below the mean-field transition temperature  $T_c^{\text{mf}}$ , significant fraction of resistivity in the resistive transition comes from the energy dissipation due to vortex motion. Working on these dynamics might provide  $T_c(H)$  indirectly and, hence,  $H_{c2}$  (Ref. 12). Since the vortex dynamics involves pins in a statistical way, it needs detailed information about the defect structure included in specimens on a submacroscopic scale. Compared with this method, on the other hand, the thermodynamic fluctuation effect provides a more direct approach to the GL

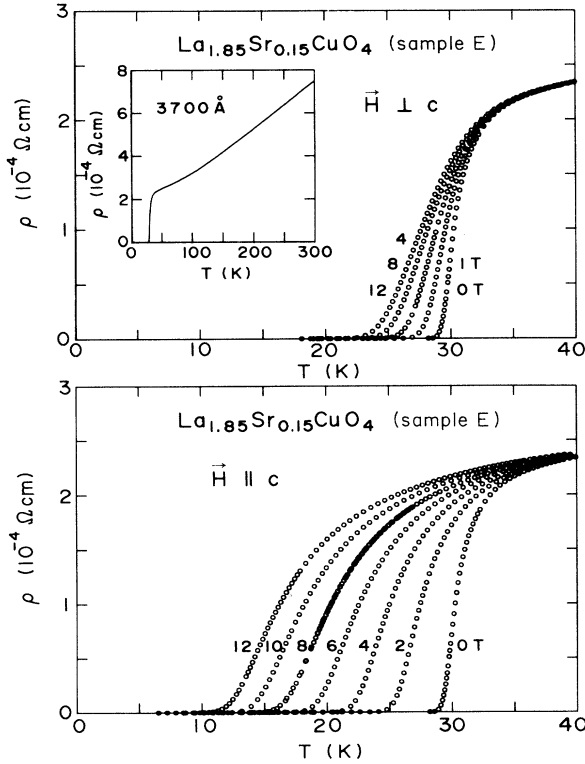


FIG. 4. Resistive transition curves for a  $\text{La}_{1.85}\text{Sr}_{0.15}\text{CuO}_4$  single-crystal thin film (sample E) under various applied magnetic fields from 1 to 12 T with the field direction perpendicular to the  $c$  axis (upper panel) and parallel to the  $c$  axis (lower panel). The inset into the upper panel shows an extended view of  $\rho(T)$ .

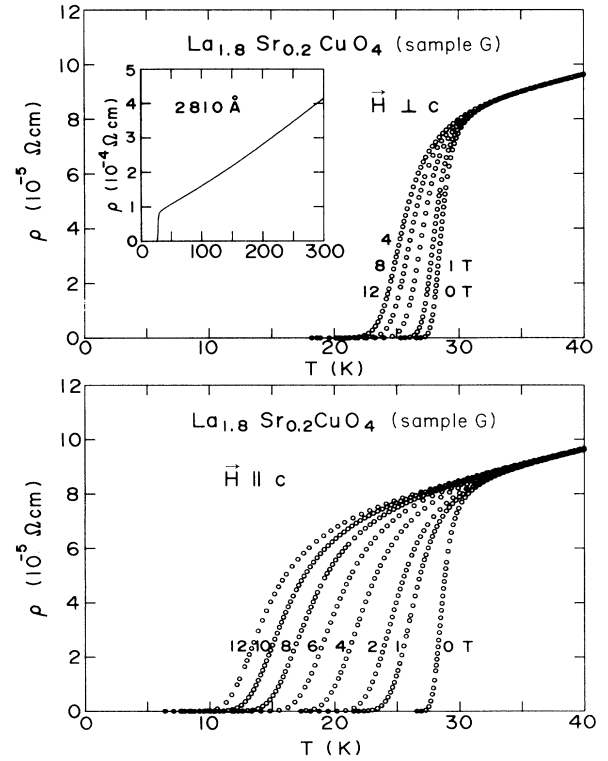


FIG. 5. Resistive transition curves for a  $\text{La}_{1.8}\text{Sr}_{0.2}\text{CuO}_4$  single-crystal thin film (sample G) under various applied magnetic fields from 1 to 12 T with the field direction perpendicular to the  $c$  axis (upper panel) and parallel to the  $c$  axis (lower panel). The inset into the upper panel shows an extended view of  $\rho(T)$ .

coherence lengths  $\xi_{GL}$ . Among the physical properties in which the thermodynamic fluctuation manifests itself, such as specific heat or magnetic susceptibility,<sup>23</sup> the experimental approach of measuring fluctuation-induced resistivity is most common because of the accuracy of measurements.<sup>24</sup>

In anisotropic materials,  $\xi_{GL}$  differs with respect to the crystallographic axes, and, therefore, single-crystalline samples are necessary to obtain anisotropic information. For this reason, it is also necessary to measure the magnetoresistance as a function of  $H$  direction, i.e., along one of the crystallographic axes. In conventional approaches, fluctuation conductivity is determined by subtracting measured resistivity from the linear extrapolation from high temperatures.<sup>24</sup> In high- $T_c$  superconductors, this method involves uncertainties to an un-negligible extent even near  $T_c$ , because the normal resistivity  $\rho_n$  does not necessarily coincide with the linear extrapolation,<sup>14</sup> and usually provides less information concerning anisotropy. As will be clear in the next section, analyzing magnetoresistance above  $T_c$  provides values for  $\xi_{GL}$ . The advantage of this method is that it needs no assumption for the normal state resistivity  $\rho_n$ .

Magnetoconductivity  $\Delta\sigma$  observed for the present

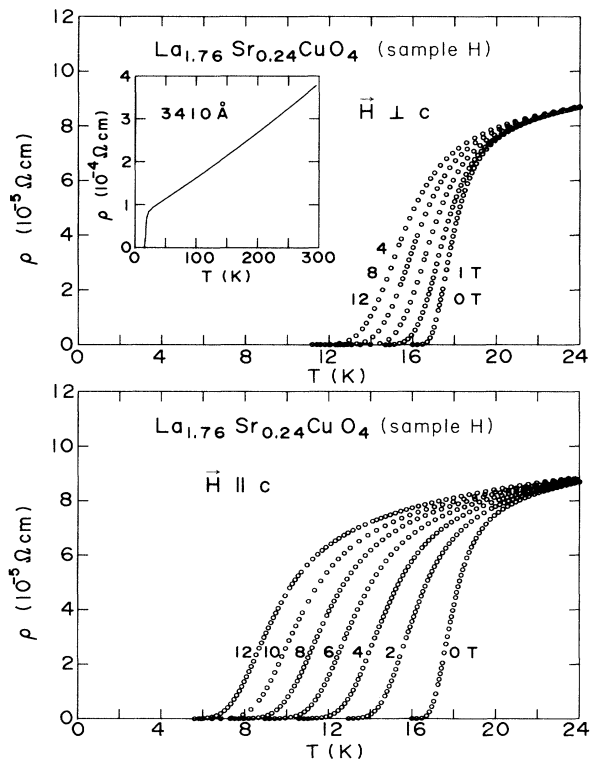


FIG. 6. Resistive transition curves for a  $\text{La}_{1.76}\text{Sr}_{0.24}\text{CuO}_4$  single-crystal thin film (sample  $H$ ) under various applied magnetic fields from 1 to 12 T with the field direction perpendicular to the  $c$  axis (upper panel) and parallel to the  $c$  axis (lower panel). The inset into the upper panel shows an extended view of  $\rho(T)$ .

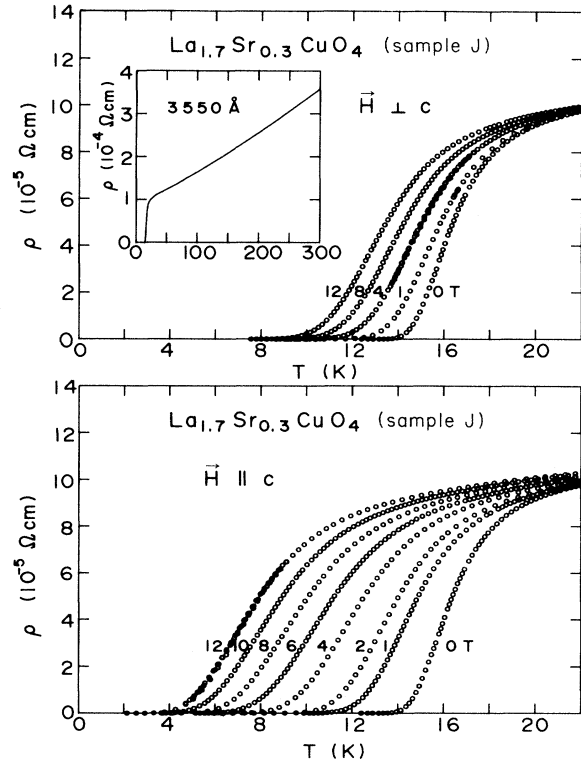


FIG. 7. Resistive transition curves for a  $\text{La}_{1.7}\text{Sr}_{0.3}\text{CuO}_4$  single-crystal thin film (sample  $J$ ) under various applied magnetic fields from 1 to 12 T with the field direction perpendicular to the  $c$  axis (upper panel) and parallel to the  $c$  axis (lower panel). The inset into the upper panel shows an extended view of  $\rho(T)$ .

$\text{La}_{2-x}\text{Sr}_x\text{CuO}_4$  samples are plotted in Fig. 9 for representative samples at selected temperatures. When compared with the  $\text{Ba}_2\text{YCu}_3\text{O}_{7-y}$  system, the resistive transition of the  $\text{La}_{2-x}\text{Sr}_x\text{CuO}_4$  system has an appreciable width of order of 1 K, which corresponds to  $\epsilon \sim 0.03$  with

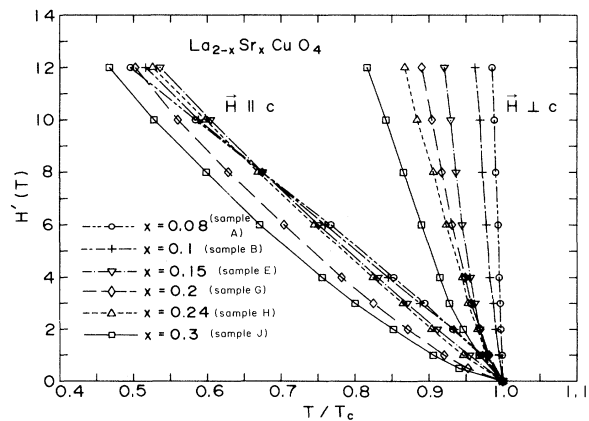


FIG. 8. Resistively determined " $H_{c2}$ " as a function of a reduced temperature  $t = T/T_c$  for  $\text{La}_{2-x}\text{Sr}_x\text{CuO}_4$  single-crystal thin films with various Sr concentrations. The details for these values are given in Table I in Sec. IV.

$\epsilon = T/T_c - 1$ , even in high quality crystals. Due to this broadness of the transition, the data too close to  $T_c$  (for example,  $\epsilon < 0.08$ ) result in unsatisfactory analytical fits. At higher temperatures, where  $\epsilon \geq 0.5$ , the accuracy of the  $\Delta\sigma$  data is not sufficient for the analysis, mainly due to the scatter in temperature data and the lack in voltage resolution in the measurements. These conditions limit the  $\epsilon$  range for analysis of  $0.05 < \epsilon < 0.5$ .

As seen in Fig. 9 the magnetoconductivity  $\Delta\sigma$  shows significant anisotropy with respect to the  $c$  axis at smaller  $x$ . At larger  $x$ , the anisotropy becomes less noticeable. For example, the anisotropy for  $\Delta\sigma$  at 33 K is 40 for  $x = 0.08$  and 4 for  $x = 0.15$ . For this and reasons mentioned above, the scatter in the  $\Delta\sigma$  data is large when  $\mathbf{H} \parallel c$ . The  $H$  dependence also changes as  $x$  increases. Except for a region close to  $T_c$ , the  $H$  dependence of  $\Delta\sigma$  is approximately quadratic or shows linear behavior in the case for  $x < 0.15$ , while in the case for  $x \geq 0.15$  it appears that  $\Delta\sigma \propto H^p$  where  $p < 1$ . The latter behavior cannot be accounted for by theories and remains to be explained.

### B. Analysis on fluctuation-induced magnetoresistance

The present analysis of the magnetoconductivity due to thermodynamic fluctuation is based on the theories by

Hikami and Larkin,<sup>25</sup> and by Aronov, Hikami, and Larkin.<sup>26</sup> There are two contributions to the superconducting fluctuation conductivity  $\Delta\sigma$ : the Aslamazov-Larkin (AL) term and the Maki-Thompson (MT) term. Each further involves two effects: the orbital effect and the Zeeman effect. In layered materials like cuprate superconductors in the present case, the orbital effect is confined within the  $\text{CuO}_2$  planes, i.e., in the case of  $\mathbf{H} \parallel c$ , while the Zeeman effect is independent of the field direction. Therefore, there are four contributions: the orbital effect AL term (ALO), the orbital effect MT term (MTO), the Zeeman effect AL term (ALZ), and the Zeeman effect MT term (MTZ). Then the field-dependent fluctuation conductivity  $\Delta\sigma(H)$  is

$$\Delta\sigma(H) = \Delta\sigma_{\text{ALO}}(H) + \Delta\sigma_{\text{MTO}}(H) + \Delta\sigma_{\text{ALZ}}(H) + \Delta\sigma_{\text{MTZ}}(H), \quad (1)$$

where  $\Delta\sigma_{\text{ALO}}(H) = \sigma_{\text{ALO}}(H) - \sigma_{\text{ALO}}(0)$  and so on. Using the relations,  $\sigma_0 = e^2/8\hbar d$ ,  $\epsilon = (T - T_c)/T_c$ ,  $\alpha = 2\xi_c^2(0)/d^2\epsilon$ , and  $h = 2e\xi_{ab}^2(0)H/\hbar c$ , each term in Eq. (1) is expressed in the following way:

$$\sigma_{\text{ALO}}(H) = \frac{\sigma_0}{2\pi\hbar^2} \int_0^{2\pi} \epsilon_k \left[ \psi(\epsilon') - \psi(\epsilon' + \frac{1}{2}) + \frac{h}{\epsilon_k} \right] d\theta, \quad (2)$$

$$\sigma_{\text{ALO}}(0) = \frac{\sigma_0}{2\epsilon\sqrt{1+2\alpha}}, \quad (3)$$

$$\sigma_{\text{MTO}}(H) = \frac{\sigma_0}{2\pi p} \int_0^{2\pi} \left[ \psi\left[\epsilon' + \frac{p}{2h}\right] - \psi(\epsilon') \right] d\theta, \quad (4)$$

$$\sigma_{\text{MTO}}(0) = -\frac{\sigma_0}{p} \ln \left[ \frac{\delta}{\alpha} \frac{1+\alpha+\sqrt{1+2\alpha}}{1+\delta+\sqrt{1+2\delta}} \right], \quad (5)$$

where

$$\epsilon' = \frac{1}{2} + \frac{\epsilon_k}{2h},$$

$$\delta = \frac{16\xi_c^2(0)k_B T \tau_\phi}{\pi d^2 \hbar},$$

$$\epsilon_k = \epsilon[1 + \alpha(1 - \cos\theta)],$$

and

$$p = \epsilon\alpha(\delta^{-1} - \alpha^{-1}),$$

with  $\psi(\epsilon')$  being the digamma function,  $\tau_\phi$  the phase relaxation time, and  $d = 6.65 \text{ \AA}$  the spacing of  $\text{CuO}_2$  layers for  $\text{La}_{2-x}\text{Sr}_x\text{CuO}_4$ . For the Zeeman effect expressions for  $\sigma_{\text{ALZ}}(H)$  and  $\sigma_{\text{MTZ}}(H)$ , which are used in calculating  $\epsilon$  dependence of each component, we use the Eqs. (5) and (12) in Ref. 26.

These expressions are derived on the basis of the Ginzburg-Landau theory applied to layered superconductors in the dirty limit. On the other hand, Bieri and Maki<sup>27</sup> recently proposed a theory for the fluctuation-induced magnetoconductivity applicable to superconductors in the clean limit. Regarding the  $\text{Ba}_2\text{YCu}_3\text{O}_{7-y}$  sys-

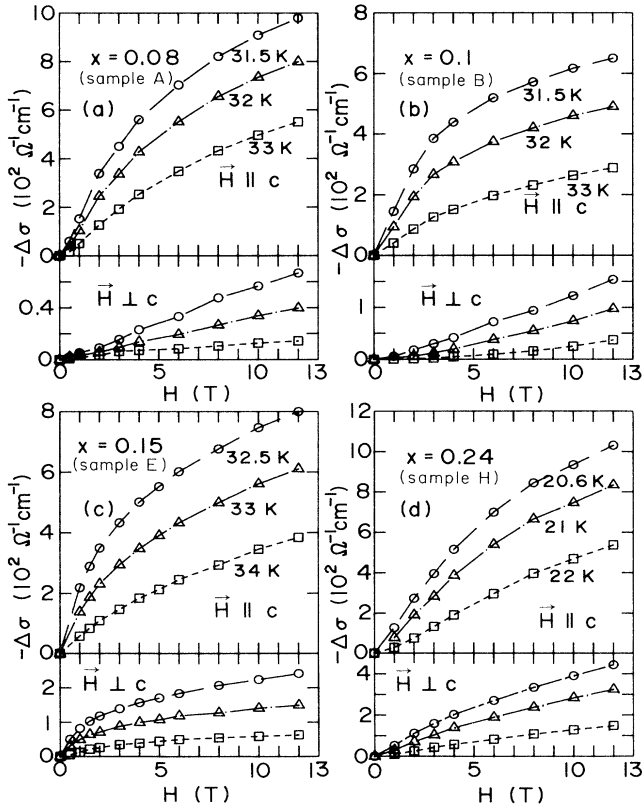


FIG. 9. Magnetoconductivity  $\Delta\sigma(H)$  for  $\text{La}_{2-x}\text{Sr}_x\text{CuO}_4$  single-crystal thin films for (a)  $x = 0.08$ , (b)  $x = 0.1$ , (c)  $x = 0.15$ , and (d)  $x = 0.24$ , with an applied field parallel and perpendicular to the  $c$  axis at several temperatures.

tem in the clean limit, they applied their theory to the experimental results, obtaining the values of  $\xi_{ab}(0) = 8.05 \sim 9.2 \text{ \AA}$  and  $\xi_c(0) = 3.36 \text{ \AA}$ , which are different by a factor of  $1.5 \sim 2$  from those obtained by using the theories of Hikami and co-workers.<sup>25,26</sup> While the  $\text{Ba}_2\text{YCu}_3\text{O}_{7-y}$  system may be regarded as being in the clean limit, it is not necessarily the case for the  $\text{La}_{2-x}\text{Sr}_x\text{CuO}_4$  system. If we temporarily assume that the Fermi velocity is of the order of  $10^7 \text{ cm/s}$  for this system,<sup>28</sup> then the mean free path  $l$  is estimated using a carrier scattering time  $\tau = 1.5 \times 10^{-14} \text{ s}$  obtained from optical measurements<sup>17</sup> to be about  $15 \text{ \AA}$  and no greater than  $30 \text{ \AA}$ , suggesting that the system can be regarded as still being in the dirty limit. Consequently, in the present study we analyze the  $\Delta\sigma$  data based on the theories by Hikami and co-workers.<sup>25,26</sup> It must be reminded here that the expression for  $\Delta\sigma_{\text{ALO}}$ , the most dominant term in the  $T$  range considered, is the same regardless of whether the system is in the clean limit or in the dirty limit.

In Fig. 10 magnetoconductivities  $\Delta\sigma_{\parallel c}$  for  $\mathbf{H}\parallel c$  and  $\Delta\sigma_{\perp c}$  for  $\mathbf{H}\perp c$  are plotted as a function of  $H$  for  $x=0.24$ . (This composition is chosen for clarity because  $\Delta\sigma_{\perp c}$  is large as compared with smaller  $x$  samples.) In the theory for the Zeeman effect magnetoconductivity, both  $\Delta\sigma_{\text{ALZ}}$

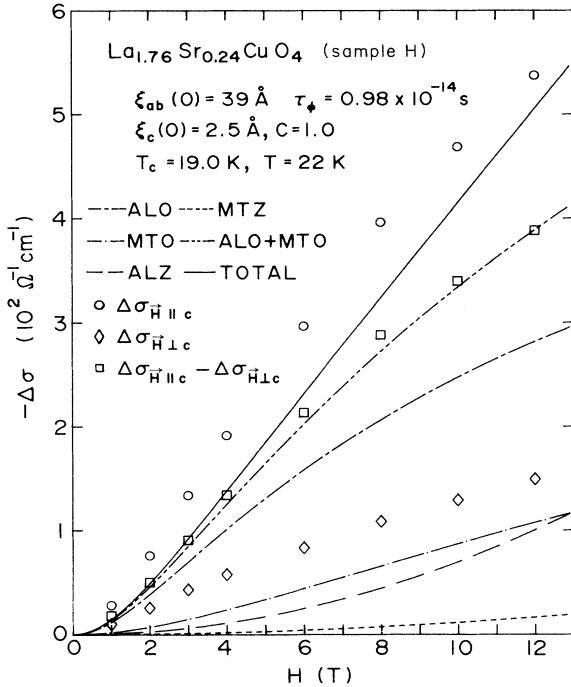


FIG. 10. Fits of Eqs. (2)–(5) and Eqs. (5) and (12) in Ref. 24 to the magnetoconductivity data for  $\text{La}_{1.76}\text{Sr}_{0.24}\text{CuO}_4$  (sample H) at 22 K. The data for  $\Delta\sigma_{H\perp c}$  are compared with the ALZ and MTZ terms to show that the low-field approximation is inappropriate in the present study. Fits are made so that the sum of the ALO and MTO terms coincide with the values for  $\Delta\sigma_{H\parallel c} - \Delta\sigma_{H\perp c}$  values. The parameters for the fits are shown in the figure.

and  $\Delta\sigma_{\text{MTZ}}$  depend on  $H$  quadratically in the low field approximation, provided that the temperature range considered is not too close to  $T_c$ . In the Zeeman effect magnetoconductivity, magnetic fields in ordinary laboratories are regarded as sufficiently low. Then the present experimental data should be viewed from this approximation. When we compare the experimental data for  $\Delta\sigma_{\perp c}$  with the theory ( $\Delta\sigma_{\text{ALZ}}$  and  $\Delta\sigma_{\text{MTZ}}$ ), it is clear that  $\Delta\sigma_{\perp c}$  exhibits linear  $H$  dependence when  $H$  exceeds 5 T rather than the quadratic dependence. (When  $H$  is low or  $\epsilon$  is large enough, we observe quadratic  $H$  dependence rather than linear dependence, for example, for  $x=0.1$  in Fig. 9.) Thus it seems that the magnetoresistance for  $\mathbf{H}\perp c$  cannot be explained solely with the theory by Aronov, Hikami, and Larkin<sup>26</sup> in the region where  $H$  is higher than a few tesla and  $T$  is very close to  $T_c$ . In order for the theory of Aronov, Hikami, and Larkin to be applicable, measurements should be performed apart from this region. In that case, however, the magnitude of  $\Delta\sigma_{\perp c}$  becomes small beyond the accuracy attainable in the present experiment. Thus the detailed analysis on  $\Delta\sigma_{\perp c}$  using the low-field approximation of  $\Delta\sigma_{\text{ALZ}}$  and  $\Delta\sigma_{\text{MTZ}}$  needs a more sophisticated experimental method, e.g., like that employed by Matsuda *et al.*<sup>13</sup>

Instead, the present study focuses on the orbital-effect terms since the analytical expressions for  $H$  dependence are available only for these terms for the time being. Therefore, we subtract the Zeeman-effect terms and, for this reason, the phase relaxation time  $\tau_\phi$  cannot be determined uniquely as in the study by Matsuda *et al.*<sup>13</sup> To obtain the values for  $\tau_\phi$ , we take, as a starting point, the values for the inelastic carrier scattering time determined from the Drude fits to the optical spectra of  $\text{La}_{2-x}\text{Sr}_x\text{CuO}_4$  single-crystal thin films,<sup>17</sup> assuming that the phase breaking mechanism in this system mostly arises from the inelastic carrier scattering. We also assume here that  $\tau_\phi$  depends on  $T$  in the same way as the carrier scattering time, i.e.,  $\tau_\phi \propto T^{-1}$ . The same argument was also applied to the  $\text{Ba}_2\text{YCu}_3\text{O}_{7-y}$  system.<sup>13</sup>

Again we assume here that the magnetoconductivity comes only from the superconducting fluctuation. Taking into account that  $\Delta\sigma_{\parallel c} = \Delta\sigma_{\text{ALO}} + \Delta\sigma_{\text{MTO}} + \Delta\sigma_{\text{ALZ}} + \Delta\sigma_{\text{MTZ}}$  and  $\Delta\sigma_{\perp c} = \Delta\sigma_{\text{ALZ}} + \Delta\sigma_{\text{MTZ}}$ , the values for the difference  $\Delta\sigma' = \Delta\sigma_{\parallel c} - \Delta\sigma_{\perp c}$  are plotted also in Fig. 10 and compared with  $\Delta\sigma_{\text{ALO}} + \Delta\sigma_{\text{MTO}}$  calculated using Eqs. (2)–(5). In Fig. 10 the values for  $\Delta\sigma_{\parallel c}$  and  $\Delta\sigma_{\perp c}$  are also plotted to show that fits are poor except for  $\Delta\sigma'$ . The calculation shows that the ALZ and MTZ terms deviate from the  $\Delta\sigma$  data more seriously as  $H$  increases.

The present method to obtain the values for  $\xi_{\text{GL}}$  is completed by fitting the theory to both the  $T$  dependence and the  $H$  dependence. More specifically, values for the out-of-plane coherence length  $\xi_c(0)$  are most dominantly determined by the  $T$  dependence of  $\Delta\sigma'$ , while values for  $\xi_{ab}(0)$  are determined by the  $H$  dependence. Figure 11 shows the results of calculations for Eqs. (2)–(5) and the Zeeman-effect terms in Ref. 26, together with the experimental data for  $\Delta\sigma'$  at  $x=0.15$ , which are to be compared. The mean-field transition temperature  $T_c$  used in

the calculation is determined primarily by this fitting of the  $T$  dependence in the same spirit as taken by Paalanen and Fiory.<sup>29</sup> Also we introduce the  $C$  parameter, first adopted by Oh *et al.*,<sup>10</sup> to normalize material-dependent variation in  $\rho(T)$  values. To obtain better fits, the procedures involved in Figs. 10 and 11 are repeated until the parameters converge. For example, the fits in Figs. 10 and 11 are the best reached by this process. In the fitting procedure, the  $T$  and  $H$  dependences play the most important and decisive role. In this sense, voids or nonsuperconducting impurities have little influence on the results, because the effect of these impurities is absorbed into the  $C$  factor. Thus, again, the essential point required for specimens in the present study is that they are completely crystallographically oriented.

In Figs. 12(a)–12(f), the fits of  $\Delta\sigma_{\text{ALO}}(\epsilon) + \Delta\sigma_{\text{MTO}}(\epsilon)$  to the experimental data  $\Delta\sigma'(\epsilon)$  are shown for  $x=0.08$  to 0.3 at  $H=1$  T and 8 T. Compared with the case for  $H=8$  T, the fits at  $H=1$  T seem less adequate. This is explained by the experimental limit in the accuracy of the  $\Delta\sigma$  data due to a small change in  $\rho$  at  $H=1$  T. As is common to all the compositions, the deviation increases as  $\epsilon$  decreases (at lower temperatures). This is presumably explained by a finite transition width, which ranges from less than 1 K to a few K in the case of  $x=0.3$ . Taking this into account, the fitting should be weighed at larger  $\epsilon$  values, e.g.,  $\epsilon > 0.1$ . In other words, the influence of a rather broad transition width, which seems inherent to the  $\text{La}_{2-x}\text{Sr}_x\text{CuO}_4$  system, is significantly reduced as  $\epsilon$  increases, providing applicability for the fluctuation analysis to other materials which are inevitably bothered by a broad transition width. As seen in Fig. 12 we can at-

tain reasonably good fits except for  $x=0.3$ , implying that the profound rounding above  $T_c$  is explained by fluctuation, especially in the case for  $x < 0.15$ .

As for  $x=0.3$  we observe a clear shoulder in  $\Delta\sigma'(\epsilon)$ , like a crossover of the dimensionality. This is, however, highly questionable when we consider that only a combination of extraordinary parameter values can explain the steep  $\epsilon$  dependence of  $\Delta\sigma$  at larger  $\epsilon$  values. This might be related to the fact that the composition  $x=0.3$  just lies on the boundary of the phase diagram of the  $\text{La}_{2-x}\text{Sr}_x\text{CuO}_4$  system,<sup>30,31</sup> which separates the superconducting region and the normal metallic region. Although we failed to find evidence of the phase segregation suspected in this system,<sup>18</sup> the behavior seen in Fig. 12(f) might admit, for the time being, no interpretation other than the lack of electrical uniformity.

Figures 13(a)–13(f) show the experimental data for  $\Delta\sigma'$  as a function of  $H$  at several  $\epsilon$  values ranging from 0.07 to 0.4 for the same compositions in Fig. 12. In Figs. 13 lines are fits of  $\Delta\sigma_{\text{ALO}}(H) + \Delta\sigma_{\text{MTO}}(H)$  to the data. The fits are improved as  $\epsilon$  approaches and increases beyond 0.1, as in the case of  $\epsilon$  dependence. The curvature of the

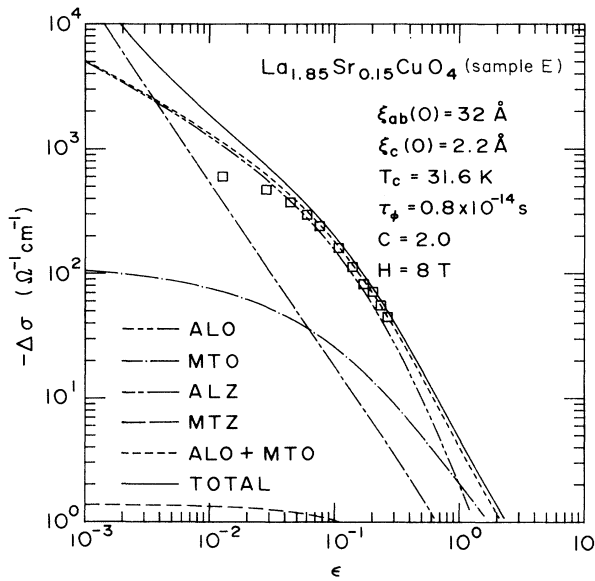


FIG. 11. Fits to temperature dependence of  $\Delta\sigma' = \Delta\sigma_{H\parallel c} - \Delta\sigma_{H\perp c}$  at  $H=8$  T for  $\text{La}_{1.85}\text{Sr}_{0.15}\text{CuO}_4$  (sample E). Lines are calculations for the ALO, MTO, ALZ, and MTZ terms using Eqs. (2)–(5) and the corresponding equations in Ref. 24. The parameters for the fits are shown in the figure.

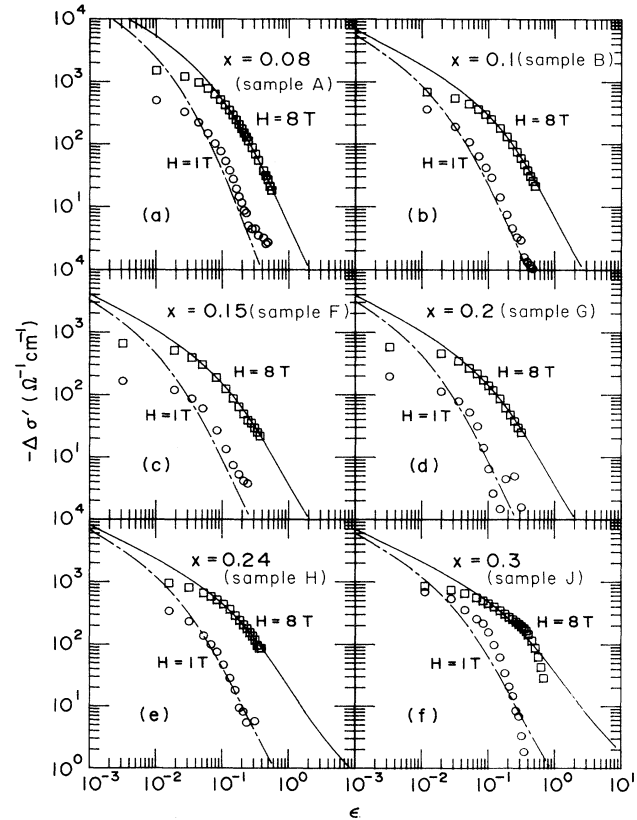


FIG. 12. Temperature dependence of  $\Delta\sigma' = \Delta\sigma_{H\parallel c} - \Delta\sigma_{H\perp c}$  for  $\text{La}_{2-x}\text{Sr}_x\text{CuO}_4$  single-crystal thin films with (a)  $x=0.08$ , (b)  $x=0.1$ , (c)  $x=0.15$ , (d)  $x=0.2$ , (e)  $x=0.24$ , and (f)  $x=0.3$  at  $H=1$  T (circles) and  $H=8$  T (squares). Lines are fits to the data using only the ALO and MTO terms. The parameters for the fits are listed in Table I.



$\Delta\sigma' - H$  curves reflects values for  $\xi_{ab}(0)$  and  $\tau_\phi$ . An increase in  $\xi_{ab}(0)$  enhances the curvature, while an increase in  $\tau_\phi$  reduces it, since the latter increases  $\Delta\sigma_{MTO}$ , which is approximately linear in  $H$  in the  $H$  region considered. The general tendency seen in the series of  $\Delta\sigma' - H$  plots and the fits to these data is that the curvature of the  $\Delta\sigma' - H$  curves gradually increases with  $x$  when  $x < 0.15$ , implying a gradual increase in  $\xi_{ab}(0)$ . When  $x > 0.15$ , this tendency becomes less apparent due to the result of

cancellation between the increase in  $\xi_{ab}(0)$  and an increase in  $\tau_\phi$ . The errors in  $\xi_{ab}(0)$  and  $\xi_c(0)$  involved in the fitting are at most  $\pm 2 \text{ \AA}$  and  $\pm 0.2 \text{ \AA}$  for  $x \leq 0.2$ , respectively. The values for  $\tau_\phi$  are adjusted around the starting values so that they give good fits to the  $\epsilon$  dependence at larger  $\epsilon$  values. The results obtained for  $\tau_\phi$  almost reproduce the original  $x$  dependence. It is also noted that the values for the  $C$  parameter range from 1 to 4. This means that the samples are generally of good quality

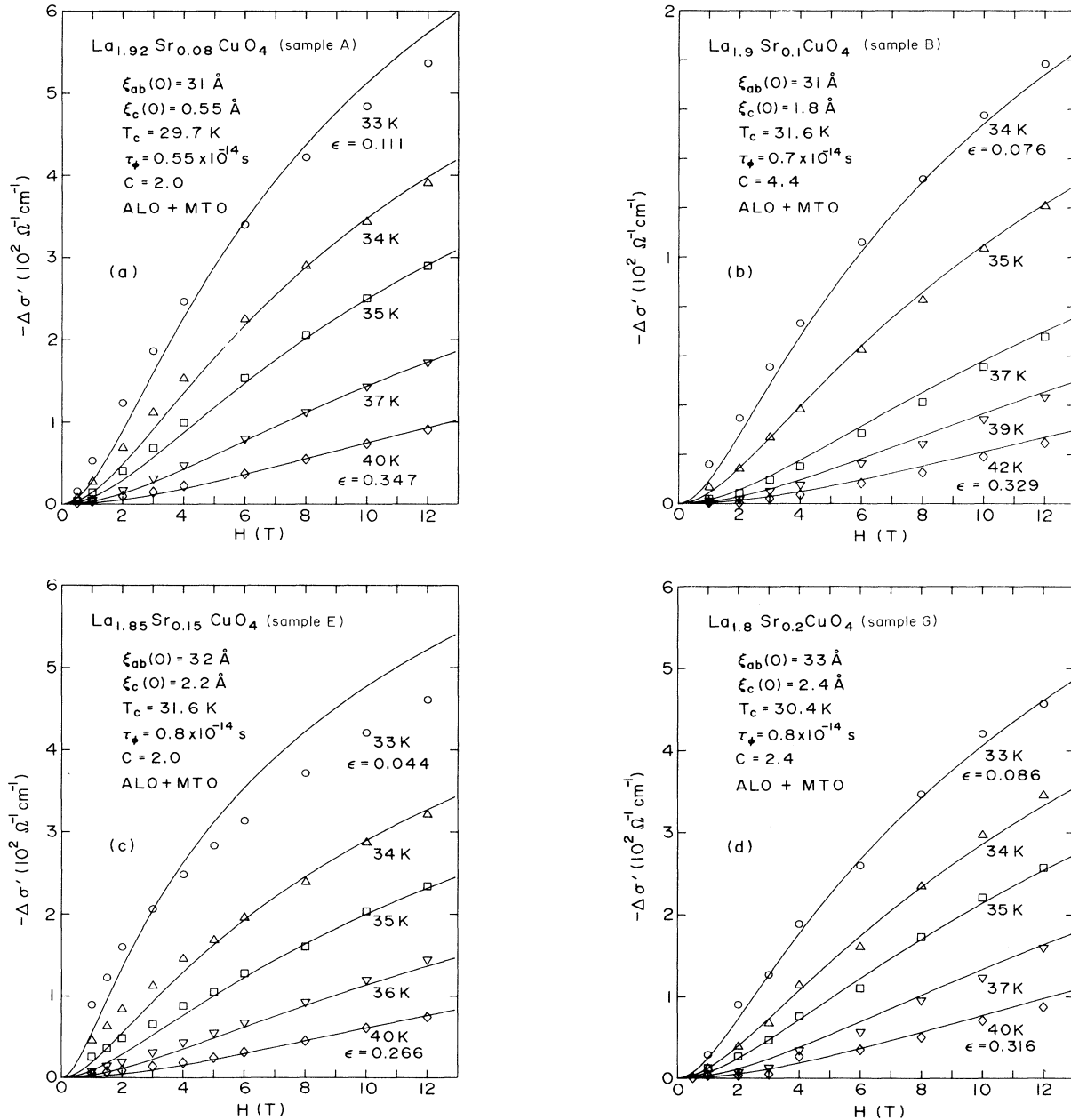


FIG. 13. Field dependence of magnetoconductivity  $\Delta\sigma' = \Delta\sigma_{H\parallel c} - \Delta\sigma_{H\perp c}$  for  $\text{La}_{2-x}\text{Sr}_x\text{CuO}_4$  single-crystal thin films with (a)  $x = 0.08$ , (b)  $x = 0.1$ , (c)  $x = 0.15$ , (d)  $x = 0.2$ , (e)  $x = 0.24$ , and (f)  $x = 0.3$  at several temperatures. The lines are the fits to the data using only the ALO and MTO terms. The parameters for the fits are listed in Table I.

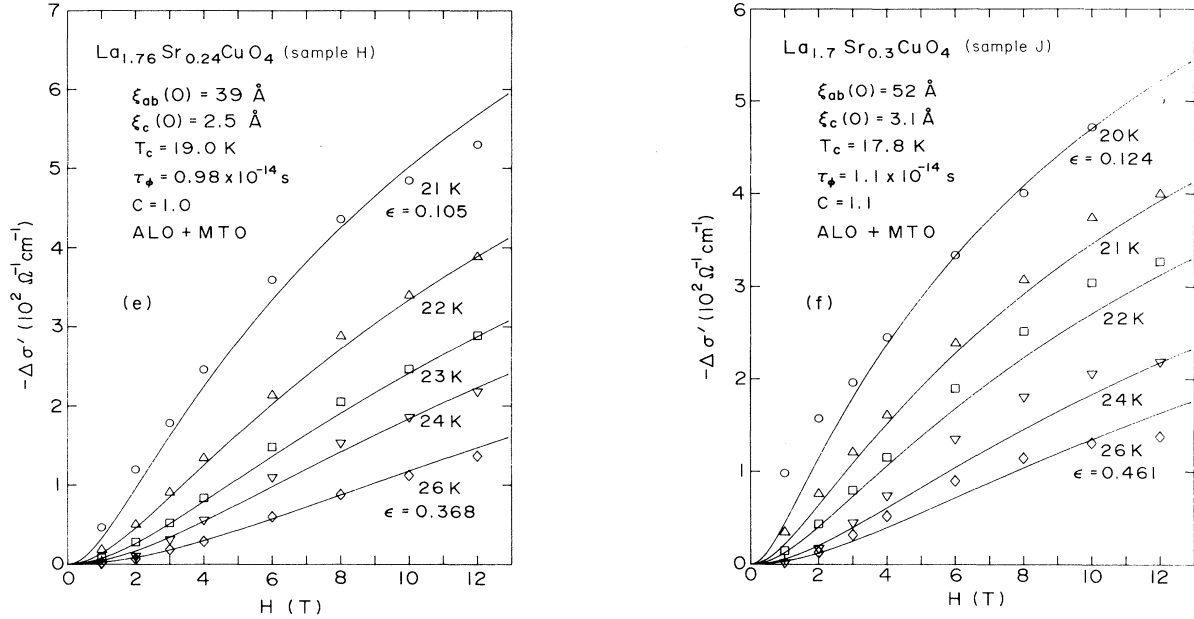


FIG. 13. (Continued).

as suggested by Matsuda *et al.*,<sup>13</sup> though there is some scatter among samples.

It should be noted here that the values for  $\tau_\phi$  for the  $\text{La}_{2-x}\text{Sr}_x\text{CuO}_4$  system is about  $1 \times 10^{-14} \text{ s}$  at 300 K, roughly corresponding to  $3 \times 10^{-14} \text{ s}$  at 100 K. Matsuda *et al.*<sup>13</sup> obtained the value of  $\tau_\phi = 1.05 \times 10^{-13} \text{ s}$ , about a factor of 3 greater than in the present case. If the same arguments hold in the present case, this result for  $\tau_\phi$  implies that there is a very strong pair-breaking mechanism in the  $\text{La}_{2-x}\text{Sr}_x\text{CuO}_4$  system. It further implies that

$T_c = 130 \text{ K}$  is expected, e.g., for  $x = 0.15$  in the absence of pair breaking. Although the pair-breaking mechanism for high- $T_c$  superconductors is not well understood at present, it, once known, provides a very important clue to the understanding of high- $T_c$  superconductivity.

From the analysis of the field-dependent fluctuation conductivity  $\Delta\sigma(H)$ , we obtain the coherence lengths  $\xi_{ab}(0)$  and  $\xi_c(0)$  for the  $\text{La}_{2-x}\text{Sr}_x\text{CuO}_4$  system with  $x$  ranging from 0.08 to 0.3. Table I lists these values together with the parameters used for the fits in Figs. 12

TABLE I. Physical properties of  $\text{La}_{2-x}\text{Sr}_x\text{CuO}_4$  single-crystal thin-film samples used in the present study. Values for the Ginzburg-Landau coherence lengths  $\xi_{ab}(0)$  and  $\xi_c(0)$ , the mean-field superconducting transition temperature  $T_c^{\text{mf}}$ , and the  $C$  parameter are determined by the fits described in Sec. IV. The values in brackets for  $\xi_{ab}(0)$ ,  $\xi_c(0)$ , and the anisotropy  $\xi_{ab}(0)/\xi_c(0)$  are determined by the conventional method using resistive transition curves, and listed here only for comparison. The errors involved are, respectively,  $\pm 2 \text{ \AA}$  and  $\pm 0.2 \text{ \AA}$  approximately for  $\xi_{ab}(0)$  and  $\xi_c(0)$ , unless otherwise noted.

Sample	$x$	$t$ [ $\text{\AA}$ ]	$\rho$ (40 K) [ $\Omega \text{ cm}$ ]	$\xi_{ab}(0)$ [ $\text{\AA}$ ]	$\xi_c(0)$ [ $\text{\AA}$ ]	$T_c$ [K]	$C$	$\tau_\phi$ (300 K) [ $10^{-14} \text{ s}$ ]	$\xi_{ab}/\xi_c$
A	0.08	3360	$4.74 \times 10^{-4}$	31	0.55	29.7	2.0	0.55	56
B	0.1	3630	$6.43 \times 10^{-4}$	[37]	[1.1]	31.6	4.4	0.7	[34]
				[37]	[3.1]				[12]
C	0.1	2780	$5.00 \times 10^{-4}$	37	1.7	25.2	2.0	0.6	22
D	0.1	3700	$2.84 \times 10^{-4}$	31.5	0.9	29.1	1.25	0.6	35
E	0.15	3700	$2.17 \times 10^{-4}$	32	2.2	31.6	2.0	0.8	14.5
				[37]	[7.1]				[5.1]
F	0.15	3350	$1.76 \times 10^{-4}$	33	2.2	31.4	2.5	0.8	15
G	0.2	2810	$9.96 \times 10^{-5}$	33	2.4	30.4	2.4	0.8	13.8
				[39]	[8.7]				[4.5]
H	0.24	3410	$1.04 \times 10^{-4}$	$39 \pm 5$	$2.5 \pm 0.3$	19.0	1.0	0.98	17.2
				[37]	[10.5]				[3.5]
J	0.3	3550	$1.16 \times 10^{-4}$	$52 \pm 10$	$3 \pm 0.5$	17.8	1.1	1.1	17
				[41]	[13.6]				[3.0]

and 13. The physical implications of the results are mentioned in the next section.

## V. DISCUSSION

### A. Resistive behavior below $T_c$

As shown, the conventional approach to the coherence length through the measurements of resistive transitions under fields is ineffective. In order to show this more clearly we briefly consider the resistive method for the coherence lengths and compare with the present results.

For conventional superconductors, values for  $H_{c2}$  are determined by measuring  $T_c(H)$  from the shift of resistive transition curves induced by an applied field. In this sense, the plots in Fig. 8 correspond to this definition. It seems useful to understand the resistive behavior below  $T_c$  by elucidating the discrepancy between such  $\xi$  values and the results obtained in the preceding section. This is easily done if we simply assume that, in Fig. 8,

$$\begin{aligned} dH_{c2}(T=T_c)/dT &\searrow \\ &= 8/[T_c(H=8\text{ T})-T_c(H=0)] , \\ -\frac{dH_{c2}^{\perp c}(T=T_c)}{dT} T_c(0) &= \frac{\Phi_0}{2\pi\xi_{ab}(0)\xi_c(0)} , \end{aligned}$$

and

$$-\frac{dH_{c2}^{\parallel c}(T=T_c)}{dT} T_c(0) = \frac{\Phi_0}{2\pi[\xi_{ab}(0)]^2} ,$$

where  $\Phi_0$  is the flux quantum. Table I also lists these results in brackets. Two features are clear. First, the value for the in-plane coherence length  $\xi_{ab}(0)$  are almost equal within a factor of 1.2 to the values obtained by the fluctuation analysis, while the out-of-plane coherence length  $\xi_c(0)$  is much larger by a factor of more than 4. Second, the values for  $\xi_{ab}(0)$  thus obtained show a gradual increase as  $x$  increases beyond 0.15, while the values for  $\xi_c(0)$  show a rapid and systematic increase with  $x$ , thus resulting in a rapid decrease in the apparent anisotropy factor. Then the most significant difference between the two estimation methods is seen in  $\xi_c(0)$ . Namely, when the shift of resistive transition curve is used, the values for  $\xi_c(0)$  are seriously overestimated. This overestimation of  $\xi$  values in high- $T_c$  superconductors is most probably associated with the flux motion dissipation. Therefore, when the resistivity  $\rho$  due to this dissipation becomes comparable to  $\rho_n$ , the shift of resistive transition is always larger than the shift of  $T_c$ .

When the broadening of resistive transition is significant, as in  $x=0.08\sim 0.15$ , the influence of the flux motion dissipation becomes less noticeable when  $T_c(H)$  is defined at a higher fraction of  $\rho_n$ . And, in this case, the values for  $\xi_{ab}(0)$  and  $\xi_c(0)$  changes depending on how  $T_c(H)$  is defined. Indeed, for example, when  $T_c(H)$  is defined at the point where  $\rho(T)=0.7\rho_n$ , the values of  $\xi_{ab}(0)=29.5\text{ \AA}$  and  $\xi_c(0)=0.52\text{ \AA}$  are obtained for  $x=0.08$ , and similarly the values of  $\xi_{ab}(0)=32.9\text{ \AA}$  and  $\xi_c(0)=4.7\text{ \AA}$  for  $x=0.15$ . These values are much closer to the values estimated from the fluctuation analysis than

those determined at  $0.5\rho_n$  (the values in brackets in Table I). From this, it is very clear that the small change in the  $T_c$  definition causes a drastic change in the coherence values, especially for  $\xi_c(0)$ . Since the flux motion dissipation is considered to prevail over the whole resistive transition region, however, we have no basis to claim which definition of this kind leads to a good approximation method for estimating accurate  $\xi$  values. Therefore, the method dealing with fluctuation-induced magnetoconductivity is more reliable for studying high- $T_c$  superconductors.

In relation to the  $T_c(H)$  definition in the resistive method, it is interesting to note that for  $x>0.15$  the values for  $\xi_{ab}(0)$  or  $\xi_c(0)$  scarcely change irrespective of the fraction value for  $\rho/\rho_n$  used by the  $T_c(H)$  definition. This is due to the parallel shift behavior seen in Figs. 5–7. Although such behavior appears free from the flux motion behavior, it is known that the thermally activated depinning of flux lines also results in a behavior of the kind seen in Figs. 5–7 (Ref. 12).

From the above discussion, values for  $\xi_{ab}(0)$  and  $\xi_c(0)$  determined resistively are larger than those determined from the fluctuation above  $T_c$ . However, this is not the case for  $x=0.24$  and 0.3, as seen in Table I. This implies that the  $H_{c2}-T$  curve has still positive curvature at lower temperatures for these composition. It further implies that, since  $T_c$  is low for these two compositions, the influence of thermally activated flux motion is significantly reduced at lower temperature and the shift of resistive transition is considered to reflect the shift of  $T_c$  to a substantial extent. The reason for the possibly positive curvature of  $H_{c2}-T$  curves for  $x=0.24$  and 0.3 may be ascribed to the Coulomb interaction effect in quasi-2D dirty superconductors.<sup>32</sup> The increase in disorder which this explanation invokes may be found in the  $\rho$  data at 40 K, where  $\rho$  is much larger than expected from carrier density or Sr doping level. Consequently for  $x>0.15$ , the resistive behavior below  $T_c$  for  $\mathbf{H}\parallel c$  suffers much less influence of dissipative flux motion than the case for  $\mathbf{H}\perp c$  at higher  $x$  values and at lower temperatures.

### B. Coherence lengths and anisotropy

Coherence lengths of superconductors is closely related to the microscopic physical parameters, at least in the framework of the Bardeen-Cooper-Schrieffer (BCS) theory, and probably in the high- $T_c$  superconductors. In Figs. 14 we plot the values for  $\xi_{ab}(0)$ ,  $\xi_c(0)$ , and anisotropy factor  $\xi_{ab}(0)/\xi_c(0)$  as a function of Sr concentration  $x$ , and the values for  $\xi_{ab}(0)$  as a function of the mean-field  $T_c^{\text{mf}}$  on a double-logarithmic scale. From the present analysis of the field-dependent fluctuation conductivity, it is revealed that the anisotropy of the electronic structure in the  $\text{La}_{2-x}\text{Sr}_x\text{CuO}_4$  system is significantly larger than the values ( $\sim 5$ ) reported previously.<sup>15</sup> In particular, for a lightly doped composition of  $x=0.08$ , the anisotropy factor exceeds 50, which value compares with that observed for the Bi-Sr-Ca-Cu-O system.<sup>4,5</sup> On the other hand, there is a significant difference in the anisotropy

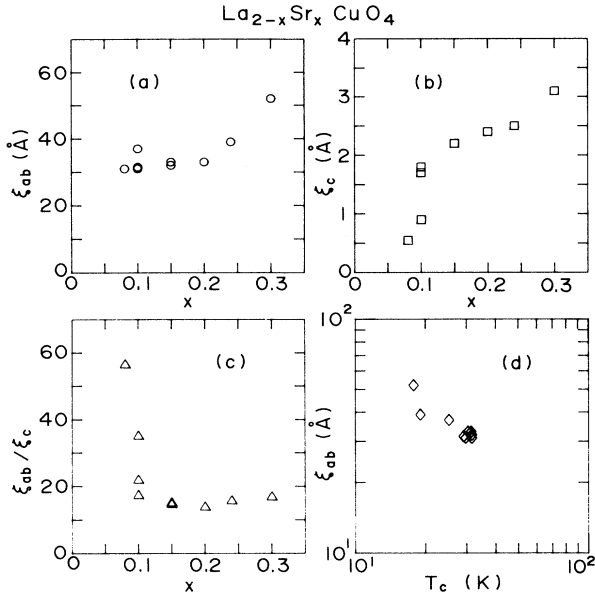


FIG. 14. (a) In-plane coherence length  $\xi_{ab}(0)$  for  $\text{La}_{2-x}\text{Sr}_x\text{CuO}_4$  single-crystal thin films as a function of Sr concentration  $x$ . (b) Out-of-plane coherence length  $\xi_c(0)$  as a function of  $x$ . (c) Anisotropy factor  $\xi_{ab}(0)/\xi_c(0)$  as a function of  $x$ . (d)  $\xi_{ab}$  vs  $T_c$  on a double-logarithmic scale, showing a negative correlation,  $\xi_{ab}(0) \propto T_c^{-1}$ .

factor between the values estimated resistively from Fig. 8 and those from the fluctuation analysis. If we take into account that  $[\xi_{ab}(0)/\xi_c(0)]^2 \sim \rho_c/\rho_{ab}$ , where  $\rho_{ab}$  is the in-plane resistivity and  $\rho_c$  is the out-of-plane resistivity, the latter anisotropy factors well correspond to the experimental values of  $\rho_c/\rho_{ab} > 100$ , which Uchida *et al.*<sup>33</sup> recently reported for the  $\text{La}_{2-x}\text{Sr}_x\text{CuO}_4$  bulk single crystals, confirming the validity of the present analysis.

As for  $\xi_{ab}(0)$ , the correlation with  $x$  is weak and the change with  $x$  can probably be explained by the variation in  $T_c$ . Figure 14(d) shows a weak but definite negative correlation with  $T_c$ , which is reminiscent of the BCS relation  $\xi_{\text{BCS}} = \hbar v_F / \pi \Delta_0 \propto \hbar v_F / k_B T_c$ , where  $\xi_{\text{BCS}}$  is the BCS coherence length.

The important point associated with the origin of high- $T_c$  superconductivity in the  $\text{La}_{2-x}\text{Sr}_x\text{CuO}_4$  system is that the system changes systematically by the Sr doping from being an insulator to a metallic nonsuperconductor through a superconducting region. Therefore it is of primary importance to find changes in physical parameters which accompany the appearance and/or disappearance of superconductivity,<sup>30</sup> seems more important and it is imperative to seek the reason why the  $\text{La}_{2-x}\text{Sr}_x\text{CuO}_4$  system loses superconductivity when

heavily doped with Sr despite the system remains metallic. The anisotropy  $\xi_{ab}(0)/\xi_c(0)$  shown in Fig. 14(d) exhibits an abrupt decrease when  $x$  increases from  $x=0.08$  and remains almost the same for  $x > 0.15$ , implying that the anisotropy itself shows essentially no change when the system undergoes a phase transition from a superconductor to a nonsuperconductor. On the other hand, the out-of-plane coherence length increases systematically from 0.55 Å at  $x=0.08$  to 3 Å at  $x=0.3$ , and it seems that, among the physical parameters shown in Fig. 14,  $\xi_c(0)$  has the closest relevance to the disappearance of superconductivity of the  $\text{La}_{2-x}\text{Sr}_x\text{CuO}_4$  system. In other words, there may be some correlation between the disappearance of superconductivity as  $x$  approaches 0.3 and the tendency that the system loses two-dimensionality. It is interesting to remind that the nuclear quadrupole resonance experiments<sup>34</sup> led to the idea that holes in  $\text{La}_{2-x}\text{Sr}_x\text{CuO}_4$  may reside at apical oxygen sites by doping. If we admit this idea, increasing carrier density may facilitate electrical conduction along the  $c$  axis, thus increasing  $\xi_c(0)$ . We believe that the present results reflect that the two-dimensionality is essential to the high- $T_c$  superconductivity in cuprates.

## VI. CONCLUSION

From the measurements of resistive transition under fields for the  $\text{La}_{2-x}\text{Sr}_x\text{CuO}_4$  system, we find that the resistive behavior changes systematically from a type of the broadening near the transition tail at lower  $x$  to a type of the parallel shift of the whole transition curves at higher  $x$ . These behaviors are ascribed to the change in the vortex dynamics accompanying the Sr doping in this system. The magnetoresistance is analyzed based on the theory of thermodynamic fluctuation above  $T_c$  for layered materials. It is found that the magnetoconductivity for  $\text{H} \parallel c$  at  $H > 1$  T cannot be explained by the theories including the Zeeman effect. The analysis of the magnetoconductivity, allowing for only the orbital AL and MT terms, provides values for  $\xi_{ab}(0)$  and  $\xi_c(0)$ . For  $x \leq 0.2$ ,  $\xi_{ab}(0)$  takes an almost constant value of 31–33 Å and tends to increase for  $x > 0.2$ , while  $\xi_c(0)$  increases systematically from 0.55 Å at  $x=0.08$  to 3 Å at  $x=0.3$ . The anisotropy  $\xi_{ab}(0)/\xi_c(0)$  estimated from these results exceeds 50 at low Sr concentration and is still higher than 15 even for  $x > 0.1$ .

## ACKNOWLEDGMENTS

The authors would like to thank H. Takagi, Y. Iye, and S. Uchida for enlightening discussions and for sending reports of their work prior to publication. They are also obliged to S. Kurihara for useful discussions, to N. Inagaki, Y. Ishii, A. Yamaji, T. Inamura, Y. Hidaka, and S. Kubo for encouragement and discussions.

\*Present address: NTT Opto-Electronics Laboratories, Nippon Telegraph and Telephone Corporation, 162 Tokai, Ibaraki 319-11, Japan.

<sup>1</sup>M. Tinkham, Phys. Rev. Lett. **61**, 1658 (1988).

<sup>2</sup>A. P. Malozemoff, T. K. Worthington, E. Zeldov, N.-C. Yeh, M. W. McElfresh, and F. Holtzberg, in *Strong Correlation and Superconductivity*, Vol. 89 of *Springer Series in Solid-State Sciences*, edited by H. Fukuyama, S. Maekawa, and A.

- P. Malozemoff (Springer-Verlag, Heidelberg, 1989), p. 349; A. P. Malozemoff, T. K. Worthington, Y. Yeshurun, F. Holtzberg, and P. H. Kes, *Phys. Rev. B* **38**, 7203 (1988).
- <sup>3</sup>Y. Yeshurun and A. P. Malozemoff, *Phys. Rev. Lett.* **60**, 2202 (1988).
- <sup>4</sup>T. T. M. Palstra, B. Batlogg, L. F. Schneemeyer, and J. V. Waszczak, *Phys. Rev. Lett.* **61**, 1662 (1988); T. T. M. Palstra, B. Batlogg, R. B. van Dover, L. F. Schneemeyer, and J. V. Waszczak, *Appl. Phys. Lett.* **54**, 763 (1989); T. T. M. Palstra, B. Batlogg, R. B. van Dover, L. F. Schneemeyer, and J. V. Waszczak, *Phys. Rev. B* **41**, 6621 (1990).
- <sup>5</sup>Y. Iye, T. Tamegai, H. Takeya, and H. Takei, *Jpn. J. Appl. Phys.* **26**, L1057 (1987); M. Oda, Y. Hidaka, M. Suzuki, and T. Murakami, *Phys. Rev. B* **38**, 252 (1988).
- <sup>6</sup>K. Kitazawa, S. Kambe, M. Naito, I. Tanaka, and H. Kojima, *Jpn. J. Appl. Phys.* **28**, L555 (1989); S. Kambe, M. Naito, K. Kitazawa, I. Tanaka, and H. Kojima, *Physica C* **160**, 243 (1989).
- <sup>7</sup>M. Suzuki and M. Hikita, *Jpn. J. Appl. Phys.* **28**, L1368 (1989).
- <sup>8</sup>T. Tsuneto, *J. Phys. Soc. Jpn.* **57**, 3499 (1988).
- <sup>9</sup>R. Ikeda, T. Ohmi, and T. Tsuneto, *J. Phys. Soc. Jpn.* **58**, 1377 (1989); R. Ikeda, *ibid.* **58**, 1906 (1989); R. Ikeda, T. Ohmi, and T. Tsuneto, *Physica C* **162-164**, 1693 (1989).
- <sup>10</sup>B. Oh, K. Char, A. D. Kent, M. Naito, M. R. Beasley, T. H. Geballe, R. H. Hammond, and A. Kapitulnik, *Phys. Rev. B* **37**, 7861 (1988).
- <sup>11</sup>U. Welp, W. K. Kwok, G. W. Crabtree, K. G. Vandervoort, and J. Z. Liu, *Phys. Rev. Lett.* **62**, 1908 (1989).
- <sup>12</sup>M. Suzuki and M. Hikita, *Phys. Rev. B* **41**, 9566 (1990).
- <sup>13</sup>Y. Matsuda, T. Hirai, S. Komiyama, T. Terashima, Y. Bando, K. Iijima, K. Yamamoto, and K. Hirata, *Phys. Rev. B* **40**, 5176 (1989); Y. Matsuda, T. Hirai, and S. Komiyama, *Solid State Commun.* **68**, 103 (1988).
- <sup>14</sup>M. Hikita and M. Suzuki, *Phys. Rev. B* **39**, 4756 (1989); **41**, 834 (1990).
- <sup>15</sup>M. Suzuki, Y. Enomoto, K. Moriwaki, and T. Murakami, *Jpn. J. Appl. Phys.* **26**, L1921 (1987); Y. Hidaka, Y. Enomoto, M. Suzuki, M. Oda, and T. Murakami, *ibid.* **26**, L377 (1987); S. Shamoto, M. Onoda, and M. Sato, *Solid State Commun.* **62**, 479 (1987).
- <sup>16</sup>Y. Iye, T. Tamegai, and S. Nakamura (unpublished).
- <sup>17</sup>M. Suzuki, *Phys. Rev. B* **39**, 2312 (1989).
- <sup>18</sup>D. R. Harshman, G. Aeppli, B. Batlogg, G. P. Espinoza, R. J. Cava, A. S. Cooper, L. W. Rupp, E. J. Ansaldo, and D. L. Williams, *Phys. Rev. Lett.* **63**, 1187 (1989).
- <sup>19</sup>J. D. Jorgensen, B. Dabrowski, Shiyou Pei, D. G. Hinks, L. Soderholm, B. Morosin, J. E. Schirber, E. L. Venturini, and D. S. Ginley, *Phys. Rev. B* **38**, 11 337 (1988).
- <sup>20</sup>H. H. Sample, *Rev. Sci. Instrum.* **53**, 1129 (1982).
- <sup>21</sup>For other samples C and D with the same nominal composition of  $x=0.1$ , field-induced transition curves are similar to those of either Fig. 2 or Fig. 3, probably reflecting some deviation of  $x$  from the nominal value.
- <sup>22</sup>M. M. Fang, V. G. Kogan, D. K. Finnemore, J. R. Clem, L. S. Chumbley, and D. E. Farrel, *Phys. Rev. B* **37**, 2334 (1988).
- <sup>23</sup>W. C. Lee, R. A. Klemm, and D. C. Johnston, *Phys. Rev. Lett.* **63**, 1012 (1989).
- <sup>24</sup>P. P. Freitas, C. C. Tsuei, and T. S. Plaskett, *Phys. Rev. B* **36**, 833 (1987); T. A. Friedmann, J. P. Rice, J. Giapintzakis, and D. M. Ginsberg, *ibid.* **39**, 4258 (1989).
- <sup>25</sup>S. Hikami and A. I. Larkin, *Mod. Phys. Lett. B* **2**, 693 (1988).
- <sup>26</sup>A. G. Aronov, S. Hikami, and A. I. Larkin, *Phys. Rev. Lett.* **62**, 965, 2336(E) (1989).
- <sup>27</sup>J. B. Bieri and K. Maki, *Phys. Rev. B* **42**, 4854 (1990).
- <sup>28</sup>To derive this value, it is simply assumed that  $n=2 \times 10^{21} \text{ cm}^{-3}$  and  $m=3m_0$ .
- <sup>29</sup>M. A. Paalanen and A. F. Fiory, *Appl. Phys. Lett.* **45**, 794 (1984).
- <sup>30</sup>J. B. Torrance, Y. Tokura, A. I. Nazzal, A. Bezing, T. C. Huang, and S. S. P. Parkin, *Phys. Rev. Lett.* **61**, 1127 (1988); J. B. Torrance, A. Bezing, A. I. Nazzal, T. C. Huang, S. S. P. Parkin, D. T. Keane, S. J. LaPlaca, P. M. Horn, and G. A. Held, *Phys. Rev. B* **40**, 8872 (1989).
- <sup>31</sup>H. Takagi, T. Ido, S. Ishibashi, M. Uota, S. Uchida, and Y. Tokura, *Phys. Rev. B* **40**, 2254 (1989).
- <sup>32</sup>S. Maekawa, H. Ebisawa, and H. Fukuyama, *J. Phys. Soc. Jpn.* **52**, 1352 (1983).
- <sup>33</sup>S. Uchida, T. Ido, H. Takagi, T. Arima, Y. Tokura, and S. Tajima, *Phys. Rev. B* **43**, 7942 (1991).
- <sup>34</sup>H. Yasuoka, T. Imai, and T. Shimizu, in *Strong Correlation and Superconductivity*, (Ref. 2), p. 254.